Eur. Phys. J. D (2015) 69: 139
DOI: 10.1140/epjd/e2015-50736-1

THE EUROPEAN PHYSICAL JOURNAL D

Regular Article

Confinement effects on an ultra-cold matter wave-packet by a square well impurity near the de-localization threshold: analytic solutions, scaling, and width properties

Ricardo Méndez-Fragoso[1] and Remigio Cabrera-Trujillo[2,a]

[1] Facultad de Ciencias, Universidad Nacional Autónoma de México, Av. Universidad 3000, Circuito Exterior S/N Delegación Coyoacán, C.P. 04510 Ciudad Universitaria, D.F. México
[2] Instituto de Ciencias Físicas, Universidad Nacional Autónoma de México, Ap. Postal 48-3, Cuernavaca, Morelos 62251, México

Received 7 October 2014 / Received in final form 16 February 2015
Published online 27 May 2015 –

Abstract. The determination of the maximum number of atoms and the density profile of an ultra-cold wave-packet, under confinement conditions by an attractive impurity near the de-localization threshold, have been an open problem in ultra-cold atom physics. In this work, we study the effect of a wave-guide impurity on an ultra-cold matter wave-packet at the threshold of de-localization. The impurity is modeled by a 1-D square well potential with depth V_0 and length $2R_0$. Coupling of the square well potential to a contact impurity of strength β at the center is also considered. The time-independent non-linear Schrödinger equation describing a Bose-Einstein condensate at the delocalization threshold is exactly solved. The density profile, maximum non-linear coupling constant, $g_{\max}$, and maximum number of atoms, $N_{\max}$, prompt to be localized by the defect potential in the ground and first excited states are also reported. It is shown that $g_{\max}$ and the density profiles become only functions of the reduced impurity size $\xi = \sqrt{V_0}R_0$. It is also found that the first excited state at the threshold of de-localization exists only for $\xi \geq \pi/(2\sqrt{2})$, always holding a lower number of atoms than the corresponding ground state for the same reduced impurity size. Also, the addition of a repulsive contact impurity leads to a non-linear coupling constant at the de-localization threshold lower than that of the square well potential. In spite of the non-linear character of the Gross-Pitaevskii equation, it is found that a general scaling-law holds for defects with the same ξ, related with the same $g_{\max}$, having the same reduced density profile in the quasi-free direction. We report the full width at half maximum for the wave-function and density profile, finding a large spread for small reduced confining conditions. Implications of these results for the determination of the wave-packet properties under confinement in atom chip and Bose-Einstein condensates are presented with the aim to motivate further experimental work.

1 Introduction

The experimental realization of Bose-Einstein condensates (BEC) allows for the study of the collective dynamics of macroscopic ensembles of atoms occupying the same single-particle quantum state [1–3]. This, in turn, has motivated the creation of new technology to study ultra-cold atoms. One of these technologies is the *atom chip* [4–6], which is capable of generating a myriad of trap geometries on an ultra-cold atom gas [7]. The atom chip plays an important role in atomic physics, enabling the cooling and trapping of a BEC in a wave-guide which is created by magnetic fields generated above patterned micro-wire circuits [8]. Atom chips have already enabled the study of matter-wave interference phenomena [9], and may improve other atomic measurement devices such as atomic clocks and global positioning systems in the future. Ideally, the BEC is loaded and trapped in the transverse ground state and is allowed to propagate freely along the third dimension. An ultra-cold matter wave-packet can then be transported through a quasi 1-D wave-guide due to the strong confinement in the two transverse dimensions [10].

The properties of a BEC at temperature $T = 0$ is well described by a mean-field approximation which results in a non-linear Schrödinger equation (NLSE) for the single-particle orbitals

$$i\partial_t \Psi = -\tfrac{1}{2}\partial_{xx}^2 \Psi + V\Psi + g\left|\Psi\right|^2 \Psi. \tag{1}$$

Here g is the non-linear coupling constant which in 1-D is given by $g = 2(N-1)a_s/a_\perp$ where a_s is the s-wave scattering length, N is the number of atoms, and $a_\perp$ is the transverse length of the wave-guide. We are using the fact that in 1-D, $g = g_{3D}/2\pi$, with g_{3D} being the 3-D coupling constant. In the case of $g \propto N$, the above NLSE is known as the Gross-Pitaevskii equation (GPE).

[a] e-mail: trujillo@fis.unam.mx

With the substitution $\Psi = e^{-i\mu t}\phi$, equation (1) takes the form

$$\mu\phi = -\tfrac{1}{2}\partial_{xx}^2\phi + V\phi + g\phi^3, \tag{2}$$

where μ is the chemical potential. Equation (2) is written in oscillator units (o.u.) with length $a_\perp = \sqrt{\hbar/m\omega_\perp}$ for a chosen transverse frequency $\omega_\perp$ and m is the mass of the individual atoms that compose the ultra-cold gas. Therefore the energy is given in units of $\hbar\omega_\perp$ and time in units of $1/\omega_\perp$, such that, in S.I. units $g^{SI} = 2\hbar^2 a_s(N-1)/m$.

At variance with the linear Schrödinger equation (LSE), the NLSE does not always admit bound states. Our goal in this work is to determine analytic solutions near the de-localization threshold and the general scaling law that determines the maximum number of atoms that are trapped by attractive defects described by 1-D potentials, when combined with transverse harmonic confinement. This corresponds to determining the limit at which the system exhibits a transition from a bound to a scattering state.

In our present treatment, the quasi-one dimensional defect potential is produced by a local modification of the transverse wave-guide, such as a constriction [11–14] or a local curvature [15–17]. Thus, the defect potential will produce an interference on the wave-packet propagation, such that atoms are lost as the wave-packet goes through the defect, as a consequence of the non-linearity in the NLSE [18,19]. As the number of atoms increases in the defect, the energy of the system will increase until becoming null with respect to the transverse trap energy [15] such that the system is no longer bound and becomes delocalized. [20,21]. This, in turn, gives us a critical or maximum value for g, i.e. a $g_{\max}$, with a maximum number of trapped atoms $N_{\max}$.

Analytic approximations for $g_{\max}$ were derived by Carr et al. [20] and Leboeuf and Pavloff [15]. Carr et al. [20] solved the 1-D NLSE for a finite square-well, finding localized solutions for $\mu < 0$ in a 1-D square well potential with a depth V_0 and width $2R_0$. The transition at $\mu = 0$ was found in terms of an approximate expression for $g_{\max}$ in terms of $\xi = \sqrt{V_0}R_0$ as

$$\frac{g_{\max}}{2\sqrt{V_0}} \approx \frac{1}{2}\left[\sqrt{2}\left(\frac{e^{-\sqrt{2}\xi}}{1+2e^{-\sqrt{2}\xi}-e^{-2\sqrt{2}\xi}}\right)+2\xi\right]. \tag{3}$$

Leboeuf and Pavloff [15] derived approximate expressions in terms of the maximum number of atoms supported by a 1-D potential based on the enclosed area defined by $\lambda = |\int_{-\infty}^{\infty} V(x)dx|$. In the low-density BEC limit, they found that $g_{\max} = 2\lambda$ stating that – in general – this was expected "to be very accurate" despite using a $V(x) \to -\lambda\delta(x)$ approximate mapping. More recent analytic work by Seaman et al. [22] showed that, for a potential $V(x) = -\beta\delta(x)$, $g_{\max} = 4\beta$ exactly. Also, Cabrera-Trujillo et al. [21] have performed a numerical analysis of $g_{\max}$ and the scaling behavior for five different impurity shapes in 1-, 2-, and 3-D with excellent results in the Thomas-Fermi (TF) region [23] ($\sqrt{V_0}R_0 \gg 1$), i.e. when the kinetic energy, in the NLSE, can be neglected.

In the present work, we provide the analytic solutions for the scaling properties under confinement conditions and extend the parameter region to low confinement conditions as compared to the numerical work of reference [21]. Furthermore, we also extend our study to include an attractive square well impurity coupled to a delta impurity at the center of the square well, all of this for 1-D. Our results agree with those of Leboeuf and Pavloff, and show that there is an overestimation by a factor of 2 in the treatment of Seaman et al. in the limit of weak potentials. Furthermore, our results show that equation (3) for $g_{\max}$ overestimates the exact value at low confinement $\sqrt{V_0}R_0 \to 0$, although we agree in the limit of strong confinement, i.e., in the TF limit.

Our work is organized with the following structure. In Section 2.1.1, we provide analytic solutions for the ground state of a square well potential at the de-localization threshold. In Section 2.1.2, we present the analytic solution for the ground state of a square well potential coupled to a contact impurity. In Section 2.2, we give the analytic solution for the case of the first excited state being at the threshold of de-localization, as well as the solution for the ground state. In Section 2.3, we discuss the profile solutions under scaling of the wave-function. We report the wave-function and density profile Full Width at Half Maximum (FWHM), in Section 2.4, and the possible experimental verification of our findings in Section 2.5. In Section 3, we provide the concluding remarks of our findings. Finally, in the Appendix we describe the numerical procedure used in this work.

2 Analytic solutions

2.1 Ground state solutions

2.1.1 Attractive square well potential

The solutions to equation (2) for an attractive impurity modeled by a finite square well potential

$$V(x) = \begin{cases} -V_0, & |x| < R_0 \\ 0, & |x| \geq R_0 \end{cases} \tag{4}$$

where $V_0 > 0$ were reported in reference [24]. In connection with a BEC they were found by Carr et al. [20]. The solution is given in terms of Jacobi elliptic functions and hyperbolic functions depending on the region considered for the square well potential and the value of the chemical potential. The even solution for $\mu < 0$ is

$$\begin{aligned}
\phi_{\rm I} &= \sqrt{\frac{2|\mu|}{g}}\,\mathrm{csch}\left(-\sqrt{2|\mu|}x+\zeta\right), \quad x < -R_0 \\
\phi_{\rm II} &= \sqrt{\frac{2m(V_0+\mu)}{(1+m)g}}\,\mathrm{sn}\left(\sqrt{\frac{2(V_0+\mu)}{(1+m)}}x+K(m)\right), \ |x| < R_0 \\
\phi_{\rm III} &= \sqrt{\frac{2|\mu|}{g}}\,\mathrm{csch}\left(\sqrt{2|\mu|}x+\zeta\right), \quad x > R_0
\end{aligned} \tag{5}$$

where sn is the sine Jacobi elliptic function with elliptic modulus m [25]. Regions I, II, and III are understood implicitly in equation (5). The traditional notation of the Jacobi elliptic functions is $\mathrm{sn}(x|m)$, but in order to simplify the notation in this work, we use $\mathrm{sn}(x)$ as its modulus m is always implicit in the function. Here, m and ζ are matching parameters between the regions and $K(m)$ is the quarter-period of sn to guarantee the parity of the wave function.

The matching conditions that equation (2) must fulfill at $x = R_0$ are

$$\phi_{\mathrm{II}}(x = R_0) = \phi_{\mathrm{III}}(x = R_0) \tag{6}$$

and

$$\phi_{x,\mathrm{II}}(x = R_0) = \phi_{x,\mathrm{III}}(x = R_0) \tag{7}$$

between regions II and III. Here $\phi_x = d\phi/dx$ and a similar condition for $x = -R_0$ between region I and II is required. These conditions determine the parameters m and ζ together with the condition that the wave function is normalized.

In the solution given by equation (5), g is a free parameter, as used in reference [20]. However, we would like to obtain the non-linear coupling constant, $g_{\max}$, when a state is near the de-localization threshold. Thus, we would like to find the $g_{\max}$ for the ground and first excited states for which $\mu = 0$. From here on, we introduce $g^n_{\max}$, where $n = 0$ and 1 to denote the ground and first excited states coupling constant, respectively.

The reader can note that in the case $\mu = 0$ the wave function in equation (5) for $|x| \geq R$ is not well defined. In that case, equation (2) could be integrated directly with $\mu = 0$, and the solution takes the form

$$\begin{aligned}
\phi_{\mathrm{I}} &= \frac{1}{a - \sqrt{g^0}x}, \quad x < -R_0 \\
\phi_{\mathrm{II}} &= \sqrt{\frac{2mV_0}{(1+m)g^0}}\,\mathrm{sn}\left(\sqrt{\frac{2V_0}{(1+m)}}x + K(m)\right), \quad |x| < R_0 \\
\phi_{\mathrm{III}} &= \frac{1}{a + \sqrt{g^0}x}, \quad x > R_0
\end{aligned} \tag{8}$$

where a and m are the matching parameters consistent with the boundary conditions, equations (6) and (7). Thus we obtain the following relationships

$$\frac{1}{a + \sqrt{g^0}R} = \sqrt{\frac{2mV_0}{(1+m)g^0}}\,\frac{\mathrm{cn}\left(\sqrt{\frac{2V_0}{(1+m)}}R_0\right)}{\mathrm{dn}\left(\sqrt{\frac{2V_0}{(1+m)}}R_0\right)} \tag{9}$$

and

$$\frac{g^0}{\left(a + \sqrt{g^0}R\right)^2} = \frac{2(1-m)V_0}{(1+m)}\sqrt{m}\,\frac{\mathrm{sn}\left(\sqrt{\frac{2V_0}{(1+m)}}R_0\right)}{\mathrm{dn}^2\left(\sqrt{\frac{2V_0}{(1+m)}}R_0\right)}. \tag{10}$$

The above equations can be solved for m, independently of the value of g^0. In fact, the value for m is determined by the following transcendental equation

$$\sqrt{m} = \mathrm{sn}\left(\sqrt{\frac{2V_0}{(1+m)}}R_0\right). \tag{11}$$

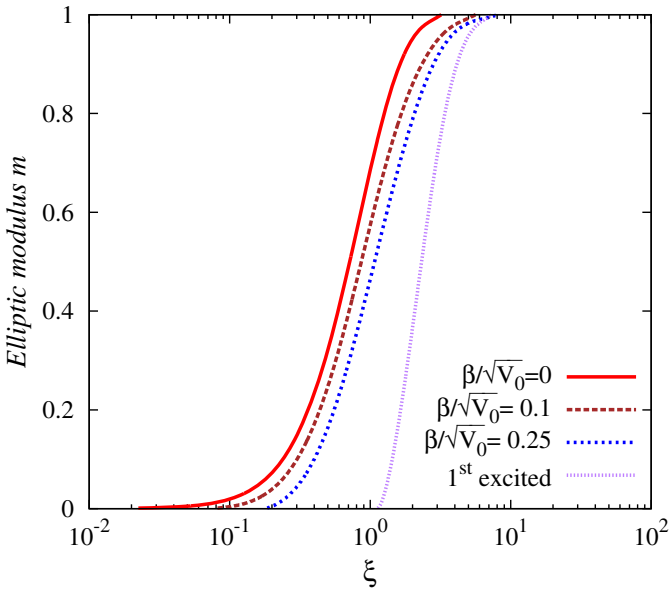

Fig. 1. Elliptic modulus m as a function of the square well potential reduced impurity size $\xi = \sqrt{V_0}R_0$. Solid line, equation (11) ($\beta = 0$, pure square potential); long-dashed line, $\beta/\sqrt{V_0} = 0.1$; short-dashed line, $\beta/\sqrt{V_0} = 0.25$; first excited state at the threshold of de-localization for the pure square well potential (dotted line). See text for details.

The behavior of m as a function of $\xi = \sqrt{V_0}R$, as given by equation (11), is shown in Figure 1 (solid line) where we observe that m is almost constant for small and large values of $\sqrt{V_0}R_0$ with a value near zero or one, respectively. The fast change in m occurs between $0.1 < \sqrt{V_0}R_0 < 2$. This indicates that for $\sqrt{V_0}R_0 > 2$, the Jacobi elliptic function becomes a hyperbolic function ($m \to 1$), and for $\sqrt{V_0}R_0 < 0.1$, it becomes a trigonometric function ($m \to 0$). So, the interesting region of study is when m takes a fast change.

Solving now equations (9) and (10) for a, we obtain

$$a = \sqrt{g^0}\left(\frac{1+m}{\sqrt{2mV_0}} - R_0\right). \tag{12}$$

The normalization of the wave function, i.e. $\int_{\infty}^{\infty} |\phi|^2 dx = 1$, results in a relation for $g^0_{\max}$

$$\begin{aligned}
\frac{g^0_{\max}}{2\sqrt{V_0}} = &-\sqrt{\frac{2}{1+m}}E\left(\sqrt{\frac{2V_0}{1+m}}R_0\middle|\, m\right) \\
&+\frac{2}{1+m}\sqrt{V_0}R_0 + \sqrt{2m},
\end{aligned} \tag{13}$$

where $E(x|m)$ is the incomplete Jacobi elliptic integral of the second kind [25].

From the previous equations, we note that the natural length of the system is $\xi = \sqrt{V_0}R_0$, which is the

reduced impurity size. The above equation and the subsequent results are more conveniently expressed in terms of the parameters ξ and $\alpha^2 = \frac{2}{1+m}$, as

$$\frac{g^0_{\max}}{2\sqrt{V_0}} = \alpha^2\xi - \alpha E(\alpha\xi|m) + \sqrt{2m}. \tag{14}$$

This equation is the exact solution to Carr's approximated expression given by equation (3). There are two interesting limits in the above result. The first one is when the potential looks like a Dirac's delta function. In the limit of $V_0 \to \infty$, $R_0 \to 0$ such that $\xi \to 0$, m is close to zero, $E(x|m) \to x$, and equation (11) takes the form

$$\sqrt{m} \approx \sqrt{\frac{2}{1+m}}\xi = \alpha\xi. \tag{15}$$

Thus, the first two terms in equation (14) cancel each other and by taking the limit when $m \to 0$ the following result is obtained

$$\frac{g^0_{\max}}{2\sqrt{V_0}} = 2\xi \quad \text{or} \quad g^0_{\max} = 4V_0R_0. \tag{16}$$

In this narrow case ($V_0 \to \infty$ and $R_0 \to 0$) the potential is equivalent to

$$V(x) = -\beta\delta(x). \tag{17}$$

To obtain β, we proceed as Leboeuf and Pavloff, i.e.

$$\int_{-\infty}^{\infty} V(x)dx = -\beta\int_{-\infty}^{\infty}\delta(x)dx = -\beta, \tag{18}$$

and by matching it to the square well potential

$$\int_{-\infty}^{\infty} V(x)dx = -V_0\int_{-R_0}^{R_0} dx = -2V_0R_0, \tag{19}$$

we find that $\beta = 2V_0R_0$ and thus equation (16) reduces to $g^0_{\max} = 2\beta$, instead of 4β, in contrast with Seaman et al. [22] but in agreement with Leboeuf and Pavloff.

The other limit is when $\xi \gg 1$. In this case, the parameter m is close to 1 and it implies that the last two terms in the equation (14) are bounded. Then the result is

$$\frac{g^0_{\max}}{2\sqrt{V_0}} = \xi \quad \text{or} \quad g^0_{\max} = 2V_0R_0, \tag{20}$$

in agreement with the result of Leboeuf and Pavloff [15] and the numerical findings of Cabrera-Trujillo et al. [21].

In Figure 2, we show the behavior of the non-linear coupling constant at the threshold of de-localization, and thus, the number of atoms trapped by the square well impurity as a function of the reduced impurity size, $\xi = \sqrt{V_0}R_0$ (solid line), as given by equation (14). The results of equations (16) and (20) can be identified from the behavior of $g^0_{\max}$ at the bottom-left and top-right of Figure 2, respectively. We note that the behavior of $g^0_{\max}$ for the square well trapping potential converges to the two correct limits when $\xi \ll 1$ and $\xi \gg 1$. The first case is known as the weak interacting gas and the second case is the strong interaction TF case. Also, for comparison, we show the analytic result of Carr et al. [20] (long-spaced dashed line), equation (3). However, Carr's et al. analytic result does not reproduce the low limit behavior, although the high limit is properly described. Carr's et al. expression is valid for $\xi > 5$ which is in the Thomas-Fermi region. In the same figure, we show the results by Cabrera-Trujillo et al. [21] obtained by means of a Gauss-Seidel (GS) [26] approach ($\times$ symbols), which we reproduce here. We note that the agreement between the numeric and analytical solution is excellent for all ξ.

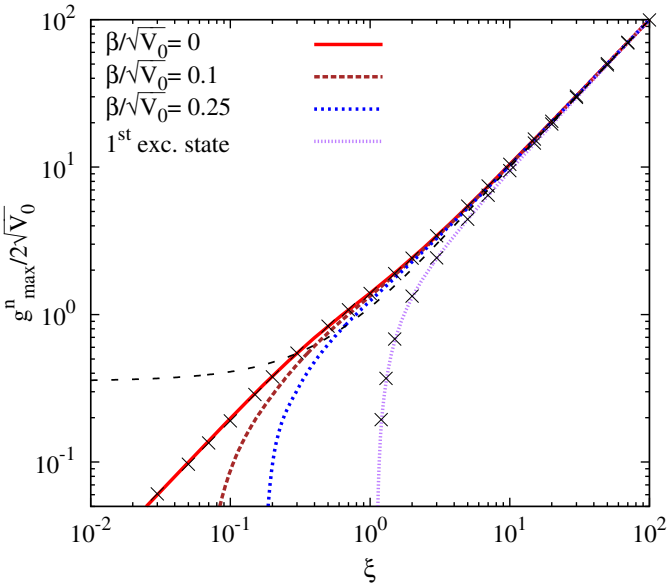

Fig. 2. Non-linear coupling constant, $g^n_{\max}/2\sqrt{V_0}$, as a function of the reduced impurity size, $\xi = \sqrt{V_0}R_0$, for the ground and first excited state ($n = 0$ and 1) of a square well potential. Solid line is the analytic solution, equation (14) ($\beta/\sqrt{V_0} = 0$). Long-spaced dashed line is Carr's approximate solution (Eq. (3)). The ($\times$) symbol is the GS numerical solution to the NLSE. The labels are the same as Figure 1.

In the Appendix, we provide an overview of the GS numerical approach for completeness of our study and as a test to confirm that we are in the correct branch for m in the Jacobi elliptic functions (see below).

2.1.2 Square well potential with a delta impurity

Let us now consider the case where there is, in addition, a contact impurity at the center of the square well potential, i.e.

$$V(x) = \begin{cases} -V_0 + \beta\delta(x), & |x| < R_0 \\ 0, & |x| \geq R_0 \end{cases} \tag{21}$$

with β constant. The solutions for each region are similar to those found previously in Section 2.1.1, but now we have to take into account the discontinuity of the wave function at the origin due to the delta impurity. In this case the wave-function satisfies

$$\phi'(0) = \beta\phi(0), \tag{22}$$

at the origin. In order to fulfill this condition, the term $K(m)$ in equation (8) is replaced by $K(m) - \gamma$, where $|\gamma| < K(m)$. The solution is thus

$$\phi_{\rm II} = \alpha\sqrt{\frac{mV_0}{g^0}}\,{\rm sn}\left(\alpha\xi|\chi| + K(m) - \gamma\right), |\chi| < 1$$
$$\phi_{I,{\rm III}} = \frac{1}{a + \sqrt{g^0}R_0|\chi|}, |\chi| > 1, \tag{23}$$

where $\chi = x/R_0$ and the parameter γ is the horizontal shift of the wave function at the origin. From the discontinuity condition (Eq. (22)), γ must satisfy the following expression

$$\alpha(1-m){\rm sn}(\gamma) = \frac{\beta}{\sqrt{V_0}}{\rm cn}(\gamma){\rm dn}(\gamma). \tag{24}$$

Notice that in the above equation γ and β have the same sign. Now, from the matching conditions, equations (6) and (7), the equation equivalent to equation (11), is

$$\sqrt{m} = {\rm sn}\left(\alpha\xi - \gamma\right). \tag{25}$$

To find $g^0_{\rm max}$, we proceed as in the previous case. For $\beta > 0$, the normalization of the wave function results in

$$\frac{g^0_{\rm max}}{2\sqrt{V_0}} = \alpha^2\xi - \alpha\left[E\left(\gamma|m\right) + E\left(\alpha\xi - \gamma|m\right)\right] + \frac{m\beta}{(1-m)\sqrt{V_0}}{\rm cn}^2(\gamma) + \sqrt{2m}. \tag{26}$$

The behavior of $g^0_{\rm max}$ for the potential given in equation (21) is characterized by the competition between the value of β and V_0. For the case of an attractive impurity, $\beta < 0$, we find that our solution does not fulfill the condition given by equation (22) for values of $\xi > -\ln(2|\beta|/\sqrt{V_0})/2$. That is, the solution does not give the correct slope at the origin. Work is in progress to find a different solution which would fulfill the proper boundary conditions at the origin.

Analogously to the case without a delta potential, the approximation for $V_0 \to \infty$ and $R_0 \to 0$, such that $\xi \to 0$ is

$$\frac{g^0_{\rm max}}{2\sqrt{V_0}} = 2\xi - \sqrt{2}\gamma. \tag{27}$$

For small values of $\beta/\sqrt{V_0}$, equation (24) is reduced to $\gamma = \beta/\sqrt{2V_0}$ giving the following relationship

$$\frac{g^0_{\rm max}}{2\sqrt{V_0}} = 2\xi - \frac{\beta}{\sqrt{V_0}} \quad \text{or} \quad g^0_{\rm max} = 4V_0R - 2\beta. \tag{28}$$

In the case of $V_0 = 0$, i.e. no square well potential but just a contact impurity, $g^0_{\rm max} = -2\beta$, in agreement with equation (16) and with Leboeuf and Pavloff [15] and in contrast to Seaman et al. [22]. From equation (28), we have that for $\xi = \beta/2\sqrt{V_0}$, $g^0_{\rm max}$ reduces to zero, and there are no more confined atoms by the impurity; thus, setting a minimum reduced well size to confine atoms in the presence of a contact impurity.

In Figure 1, we show the corresponding m values fulfilled by equations (24) and (25) for $\beta/\sqrt{V_0} = 0.1$ (long-dashed line) and $\beta/\sqrt{V_0} = 0.25$ (short-dashed line). Note that the value of m is lower for the same reduced impurity size, ξ, than that with no-contact impurity in the square well potential.

In Figure 2, we show the non-linear coupling constant when there is a repulsive delta impurity at the center of an attractive square well potential as a function of ξ for different values of $\beta/\sqrt{V_0}$. As the reader can note in Figure 2, the value of $g^0_{\rm max}/2\sqrt{V_0}$ decreases dramatically when ξ approaches to zero; that is, there is a competition between an attractive square well and a repulsive delta impurity such that the number of trapped atoms decreases dramatically. In the limit, $\xi \to \infty$, there is no significant change, up to a phase shift in the wave function and the result of equation (20) holds. In this case the effect of the delta impurity is minimal and we are in the TF region where the square well trap dominates.

2.2 First excited state for a square well potential

We now proceed to find the solution to the first excited state at the threshold of de-localization, i.e. the odd solution with $\mu = 0$, equivalent to equation (8). In this case we have

$$\phi_{\rm I} = -\frac{1}{a - \sqrt{g^1}R_0\chi}, \ \chi < -1,$$
$$\phi_{\rm II} = \alpha\sqrt{\frac{m_eV_0}{g^1}}\,{\rm sn}\left(\alpha\xi\chi\right), \ |\chi| < 1,$$
$$\phi_{\rm III} = \frac{1}{a + \sqrt{g^1}R_0\chi}, \ \chi > 1, \tag{29}$$

where now m_e is the Jacobi elliptic modulus for the excited state. The parameters a and m_e are selected to satisfy the matching conditions of equations (6) and (7) giving the following result:

$${\rm sn}^2\left(\alpha_e\xi\right) = \frac{1}{1+m_e}, \tag{30}$$

where $\alpha_e^2 = 2/(1+m_e)$ and the argument of the Jacobi elliptic function must be in the range $K(m_e) < \alpha_e\xi < 2K(m_e)$. This implies that the minimum value of the argument is $\pi/2$, and hence the smallest value of ξ is $\pi/(2\sqrt{2})$.

As in the case for the ground state at the threshold of de-localization, the normalization of the wave function gives the value for $g^1_{\rm max}$ in terms of the reduced impurity size of the square well potential

$$\frac{g^1_{\rm max}}{2\sqrt{V_0}} = \alpha_e^2\xi - \alpha_eE(\alpha_e\xi|m_e) + \frac{\sqrt{2m_e}}{1+m_e}. \tag{31}$$

When $\xi = \pi/2\sqrt{2}$, the elliptic modulus is $m_e = 0$ such that $g^1_{\rm max} = 0$ and when $\xi \gg 1$, the maximum coupling constant, $g^1_{\rm max}/2\sqrt{V_0} = \xi$, similar to the ground state case

and thus giving the same result as the TF approximation for strong confinement.

We proceed to calculate the energy of the ground state once the value of $g^1_{\max}$ is determined for the excited state at the threshold of de-localization. In this case we use equation (5) for the ground state and the matching conditions in equations (6) and (7), with the corresponding normalization of the wave function in order to get the value of m_g and $\eta = |\mu|/V_0$. This process gives the following system of equations:

$$\mathrm{sn}^2\left(\alpha_g \xi \sqrt{1-\eta}\right) = \frac{m_g+\eta}{1+m_g\eta}, \tag{32}$$

$$\frac{g^1_{\max}}{2\sqrt{V_0}} = \alpha_g^2(1-\eta)\xi - \alpha_g\sqrt{1-\eta}E(\alpha_g\sqrt{1-\eta}\xi|m_g) - \sqrt{2\eta_g} + \sqrt{\frac{2(m_g+\eta)}{1+m_g\eta}}, \tag{33}$$

where $g^1_{\max}$ is given by equation (31) and m_g is the corresponding Jacobi elliptic modulus for the ground state. Notice that η is in the interval $[0,1]$, and that m_g for the ground state is not the same as the one for the excited state, m_e, for a given $\xi = \sqrt{V_0}R_0$.

In Figure 1, we show the elliptic modulus m_e as a function of the reduced impurity size ξ for the first excited state (dotted line). Note the threshold is at $\xi = \pi/2\sqrt{2}$ and that the elliptic modulus, m_e, is lower for the same ξ than the corresponding m_g for the ground state at the threshold of de-localization.

In Figure 2, we show the corresponding coupling constant $g^1_{\max}/2\sqrt{V_0}$ as a function of ξ for the case when the first excited state is at the threshold of de-localization (dotted line). Note that for the case of the first excited state at the threshold of de-localization, the existence of the first excited state appears only for $\xi \geq \pi/2\sqrt{2}$. For lower values of ξ there exist only the ground state, as expected, since the well can hold only one state for that condition; that is, $g^1_{\max} \ll 1$ and the system behaves as in the usual delta impurity for the LSE. The second excited state, at its threshold, has the same behavior as the first excited state but can only exist for $\xi \geq \pi/\sqrt{2}$. In general, according to equations (11) and (30) the subsequent excited states can only exist for $\xi = n\pi/2\sqrt{2}$, where n is the nth excited state ($n = 0, 1, 2, \ldots$).

In Figure 3, we show the ground state bound energy, $|\eta|/V_0$, as a function of the reduced impurity size $\xi = \sqrt{V_0}R_0$ when the first excited state is at the threshold of de-localization. Note that for $\xi < \pi/2\sqrt{2}$ there is no longer a first excited state and the ground state becomes the only existing state, as mentioned above. These results can easily be understood from the LSE, i.e., for $g = 0$, the analytic solution for the first excited state at threshold gives $\sqrt{V_0}R_0 = \xi = \pi/2\sqrt{2}$ and $\eta = |\mu|/V_0 = 0.646437$ for the LSE, in agreement with our results. In Figure 3, we note that as ξ increases, $\eta \to 0$ meaning that the ground and excited states get closer as the number of particles increases and its energy approaches the threshold of de-localization, i.e. $\eta \to 0$.

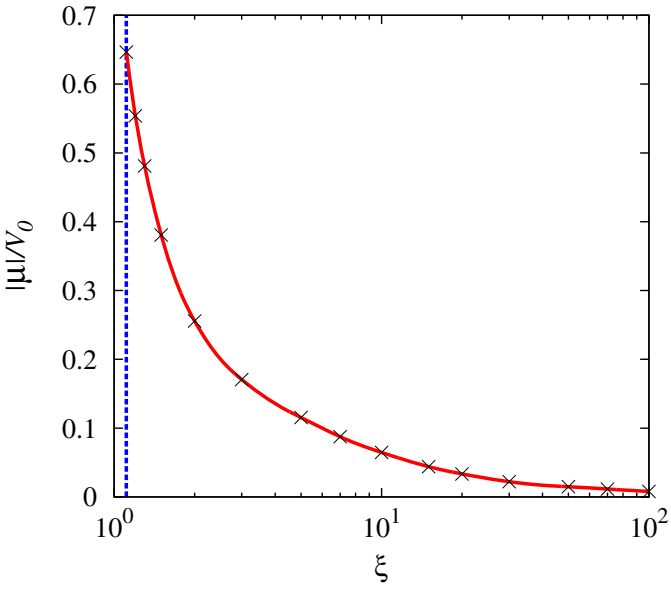

Fig. 3. Ground state bound energy, $|\mu|/V_0$, as a function of the reduced impurity size $\xi = \sqrt{V_0}R_0$ when the first excited state is at the threshold of de-localization. Solid line, analytic solution; × symbols, GS numeric solution. The vertical dash line is at $\xi = \pi/2\sqrt{2}$ which correspond to $g^1_{\max} = 0$.

For reference, in Tables 1 and 2, we provide the numerical values for the Jacobi elliptic modulus m, the reduced impurity size ξ, the non-linear coupling constant $g^n_{\max}$, and the horizontal shift parameter, γ, for several values of $\beta/\sqrt{V_0}$ for the ground and first excited states. This is because in the process of constructing the figures we have found that m can be in different branches of the quarter period $K(m)$ due to the periodicity of the Jacobi elliptic functions, complicating the numerical analysis of the analytic solutions. For this reason we have provided in the Appendix an overview of the Gauss-Seidel numerical approach, as a guide, to find the correct branch of m and to compare with the analytic solution.

2.3 Universal scaling

From the analytic solutions, equations (5), (8), (23), and (29) we note that by making the change of variables $\xi = \sqrt{V_0}R_0$, $\chi = x/R_0$, $\bar{V}(\chi) = V(\chi)/V_0$, $\bar{g} = g/2\sqrt{V_0}$, and $\bar{\phi} = \phi/\sqrt{R_0}$, the NLSE can be rewritten as

$$\left[-\frac{1}{2\xi^2}\frac{d^2}{d\chi^2} + \bar{V}(\chi) + \frac{2\bar{g}}{\xi}\bar{\phi}^2\right]\bar{\phi} = \eta\bar{\phi} \tag{34}$$

with the normalization condition given by

$$\int_{-\infty}^{\infty} \bar{\phi}^2 d\chi = 1. \tag{35}$$

This equation has the advantage that for a given value of ξ, i.e., given a reduced impurity size, the threshold of de-localization is reached by just increasing $\bar{g}$. This is particularly important when using numerical methods, as is discussed

Table 1. Values for the elliptic modulus, m, reduced impurity size $\xi = \sqrt{V_0}R_0$, shift parameter γ, and non-linear coupling constant $g^0_{\max}$ for the ground state with and without a contact potential with strength β.

	$\frac{\beta}{\sqrt{V_0}} = 0$		$\frac{\beta}{\sqrt{V_0}} = 0.1$			$\frac{\beta}{\sqrt{V_0}} = 0.25$		
m	ξ	$\frac{g^0_{\max}}{2\sqrt{V_0}}$	ξ	$\frac{g^0_{\max}}{2\sqrt{V_0}}$	γ	ξ	$\frac{g_{\max}}{2\sqrt{V_0}}$	γ
0.001	0.0224	0.0447	0.0818	0.0448	0.0840	0.1849	0.0450	0.2297
0.006	0.0550	0.1095	0.1101	0.1101	0.0777	0.2047	0.1110	0.2111
0.035	0.1354	0.2647	0.1911	0.2683	0.0774	0.2812	0.2736	0.2027
0.070	0.1960	0.3748	0.2551	0.3823	0.0808	0.3486	0.3932	0.2086
0.150	0.3027	0.5518	0.3715	0.5694	0.0907	0.4780	0.5949	0.2311
0.230	0.3959	0.6901	0.4768	0.7198	0.1031	0.5998	0.7625	0.2600
0.300	0.4750	0.7978	0.5686	0.8405	0.1161	0.7090	0.9009	0.2903
0.400	0.5905	0.9435	0.7076	1.0097	0.1399	0.8784	1.1009	0.3441
0.500	0.7154	1.0899	0.8649	1.1885	0.1727	1.0745	1.3189	0.4147
0.600	0.8574	1.2474	1.0546	1.3937	0.2204	1.3138	1.5742	0.5102
0.700	1.0296	1.4305	1.3025	1.6526	0.2960	1.6242	1.8963	0.6449
0.800	1.2590	1.6673	1.6681	2.0256	0.4312	2.0653	2.3456	0.8499
0.900	1.6312	2.0438	2.3400	2.7021	0.7272	2.8250	3.1109	1.2248
0.920	1.7478	2.1610	2.5650	2.9277	0.8340	3.0725	3.3592	1.3520
0.970	2.2507	2.6648	3.5751	3.9389	1.3344	4.2210	4.5094	1.9852
0.990	2.8050	3.2192	4.7528	5.1167	1.9527	6.0224	6.3121	3.2255

Table 2. Same as Table 1 for the first excited state at the threshold of de-localization for only the square well potential. In addition, we report the values of m_g and η for the corresponding ground state.

m_1	ξ	$\frac{g^1_{\max}}{2\sqrt{V_0}}$	m_g	η
0.0	1.1107	0.0	0.0	0.64644
0.001	1.1339	0.0458	0.00071	0.64637
0.006	1.1707	0.1162	0.14087	0.59255
0.035	1.2755	0.3034	0.35528	0.50747
0.070	1.3659	0.4520	0.48847	0.45212
0.150	1.5427	0.7168	0.66693	0.37329
0.230	1.7095	0.9437	0.77337	0.32191
0.300	1.8568	1.1309	0.83688	0.28831
0.400	2.0777	1.3955	0.89905	0.25123
0.500	2.3210	1.6712	0.93970	0.22224
0.600	2.6012	1.9754	0.96631	0.19821
0.700	2.9430	2.3348	0.98326	0.17703
0.800	3.4004	2.8044	0.99336	0.15675
0.900	4.1440	3.5554	0.99850	0.13412
0.920	4.3772	3.7895	0.99905	0.12860
0.970	5.3828	4.7967	0.99987	0.10992
0.990	6.4914	5.9056	0.99998	0.09564

in the Appendix; however, more important is the fact that when making $\tilde{\phi} = \sqrt{\frac{g}{V_0}}\phi$, the non-linear coupling term becomes one, that is, the NLSE becomes

$$\left[-\frac{1}{2\xi^2}\frac{d^2}{d\chi^2} + \bar{V}(\chi) + \tilde{\phi}^2\right]\tilde{\phi} = \eta\tilde{\phi} \tag{36}$$

with the normalization condition given by

$$\int_{-\infty}^{\infty}\tilde{\phi}^2 d\chi = \frac{g}{V_0 R_0}. \tag{37}$$

equation (34) or (36) shows that two different impurities with the same ξ value, would have the same reduced wave-function, $\bar{\phi}$, and reduced $\bar{g}$, although the number of particles is different for the same ground or excited state. The use of equation (36) is more cumbersome in numerical calculations since g has to be known *a priori* to normalize the wave-function.

The advantage of the scaling is that now the impurity strength is

$$\bar{V}(\chi) = \begin{cases} -1\ , |\chi| < 1 \\ 0\ , |\chi| \geq 1 \end{cases} \tag{38}$$

and for numerical purposes all the quantities are simplified.

In Figure 4, we show the reduced wave-function $\bar{\phi}$ for several delta impurity strengths $\beta/\sqrt{V_0}$ that shows the scaling property. Note the effect of the delta impurity on the continuity of the wave function at the origin. Furthermore, as $\beta/\sqrt{V_0}$ increases and ξ is reduced, thus a larger tunneling probability is found.

In Figure 5, we show the ground state and first excited state wave-functions, as a function of $\chi = x/R_0$ when the excited state is at the threshold of de-localization for a square well potential with $\xi = 2.6012$. The corresponding $g^1_{\max}/2\sqrt{V_0}$ value is 1.9754 for the first excited state which produces a ground state with a value for the chemical potential of $\mu = -0.19821\,V_0$. The ground state closely resembles the shape of the trapping potential; however the excited state has a large tunneling tail as a consequence of being at the de-localization threshold.

2.4 Full width half maximum

One of the properties we can check immediately with our solutions is the width of the wave-packet. Since we are reporting solutions at the threshold of de-localization, and

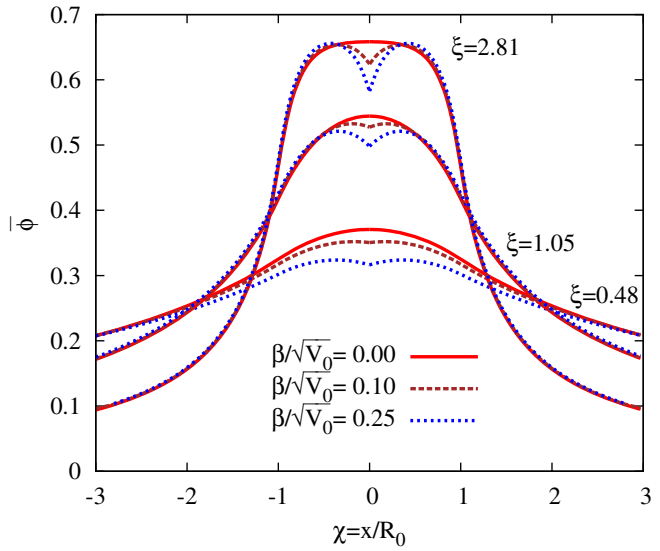

Fig. 4. Scaled ground state wave function, $\bar{\phi}$, for the square well potential with a delta impurity at the center as a function of $\chi = x/R_0$ for several values of the delta impurity strength, $\beta/\sqrt{V_0}$, and reduced impurity size ξ. The labels are the same as Figure 1.

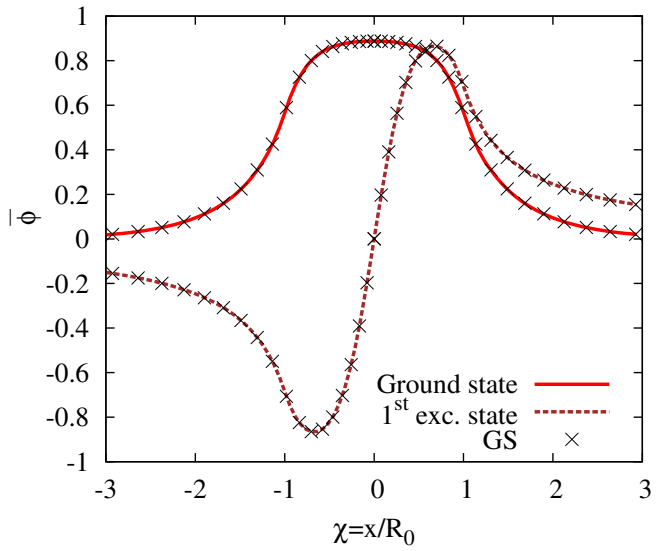

Fig. 5. Reduced wave function $\bar{\phi}$ for the ground and first excited state for a square well potential for $\xi = \sqrt{V_0}R_0 = 2.6012$ when the first excited state is at the threshold of de-localization. Continuum line: exact results; × symbol: numerical GS results.

although they are square-integrable, the term $\langle x^n \rangle$ diverges for $n > 1$, making it impossible to calculate any standard deviation $\Delta x = \sqrt{\langle x^2 \rangle - \langle x \rangle^2}$; however, we can still say how the wave-packet is spread out by reporting the Full Width at Half Maximum (FWHM) for the wave-function and for the density profile. From the analytic solutions, we determine $x_{\rm FWHM}$ for which the wave-function or density profile is half the value than when at the maximum peak. This defines the width as $\Delta x = 2x_{\rm FWHM}$.

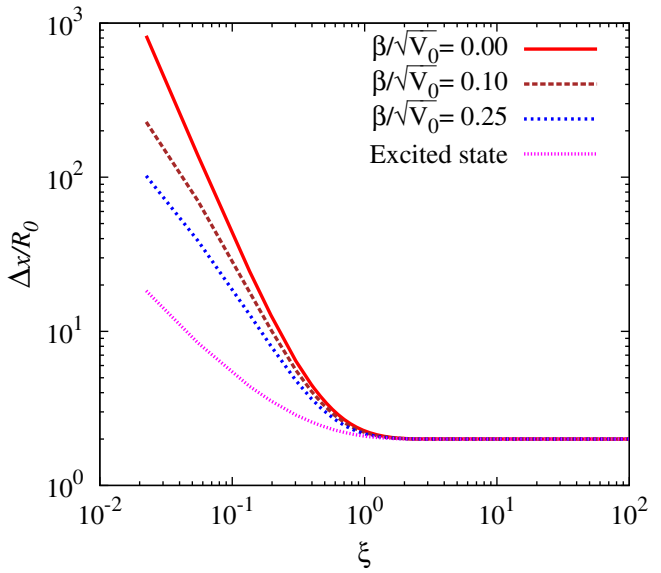

Fig. 6. Density profile width, $\Delta x/R_0$, as a function of the reduced impurity size $\xi = \sqrt{V_0}R_0$ for the ground state with and without a repulsive contact impurity at the center and also for the first excited state at the threshold of de-localization for only the square well potential. The labels are the same as in Figure 1.

For the ground state at the threshold of de-localization, we find that the width for the wave-function is

$$\frac{\Delta x}{R_0} = 2 + \frac{4}{\alpha\xi\sqrt{m}}\left(1 - \frac{1}{\alpha\sqrt{2}}\right) \tag{39}$$

and for the density profile

$$\frac{\Delta x}{R_0} = 2 + \frac{2\sqrt{2}}{\alpha\xi\sqrt{m}}\left(1 - \frac{1}{\alpha}\right). \tag{40}$$

Thus, as expected, the density profile width is narrower than that of the wave-function and it tends to be the width of the squared well, $2R_0$, as $\xi \to \infty$ in both cases, i.e. the TF limit.

Interestingly, we find that for the square-well potential with the repulsive contact impurity at the center and for the case when the excited state is at threshold, the wave-functions and density profile width are described by the same equations (39) and (40) by replacing the corresponding Jacobi elliptic modulus m with the respective one given in Tables 1 and 2.

In Figure 6, we show the density profile width as a function of the reduced impurity size $\xi = \sqrt{V_0}R_0$ for the ground state at the threshold of de-localization for $\beta/\sqrt{V_0} = 0$ (solid line), 0.1 (long-dashed line), 0.25 (short-dashed line), and for the case when the excited state is at the threshold of de-localization (dotted line). For $\xi > 2$ we find that the BEC is confined within the walls of the square well impurity. For $\xi < 2$, the BEC starts to spill over and occupies a very large size with respect to the confining impurity size, thus getting completely de-localized. Let us note that by increasing the strength of the repulsive contact impurity, the density profile of the BEC becomes

more localized for the same reduced impurity size ξ, but with fewer particles. Also, when the first excited state is at the threshold of de-localization it is more compact than the corresponding ground state for the same reduced impurity size. This is due to the fact that, at the threshold of de-localization, the first excited state has fewer particles than the ground state.

2.5 Experimental feasibility

As an example to investigate whether our findings on the density profile and the maximum number of atoms trapped by an impurity in a wave-guide can be discerned in an atom chip, let us consider ^{87}Rb atoms with $a_s = 100a_0$, as in the experiment of reference [27] moving on an atom chip. The NLSE in physical units is [3]

$$\left\{-\frac{\hbar^2}{2m}\nabla^2 + V_{trap}(\mathbf{r}) + \frac{4\pi\hbar^2 a_s(N-1)}{m}|\Psi_0(\mathbf{r})|^2\right\}\Psi_0(\mathbf{r}) = \varepsilon_0\Psi_0(\mathbf{r}). \quad (41)$$

We consider a wave-guide that produces a 1-D "cigar" shape BEC by means of a transverse harmonic confining potential

$$V_{trap}(x,y,z) = V_{trap}(x) + \frac{1}{2}m\omega_\perp^2(y^2+z^2) \quad (42)$$

with transverse length scale $a_\perp = \sqrt{\hbar/m\omega_\perp}$.

For the case that $a_\perp = 1.222\times10^{-4}$ cm $= 23100a_0$ typical for an atom chip, the non-linear coupling constant is then $g = 0.008658(N-1)$. Thus, for R_0 covering the range from 0.01 to 100 o.u., the physical values of the trap would correspond to a physical extension between 0.0122 and 122 μm. Similarly, for V_0 covering the range from 0.01 to 100 o.u., this corresponds to traps depths of 0.04 to 400 nK, which are values within the range of the experiment. The values reported in Figure 2 thus correspond to a range for ξ from 0.01 till 100 and thus to a number of atoms trapped from few atoms to 2.3×10^6 atoms, which are typically found in atom chips wave guides.

Thus, the challenge is the experimental determination of the number of trapped atoms and the shape of the BEC at the curve or bending on a wave-guide and it would provide indications as if it is in its ground state or excited state or if there is a contact impurity at the center of the curve. Also, the width of the density profile would determine the reduced impurity size on the wave-guide and thus characterize the defect in the wave-guide.

3 Concluding remarks

The maximum number of atoms that a square well potential trap can hold has been obtained analytically in this work for the ground and first excited states of an ensemble of cold atoms on a 1-D wave-guide. Similar to the linear Schrödinger equation, the non-linear Schrödinger equation has an excited state only for a potential well size/depth value higher than a critical minimum. We find that $\xi = \sqrt{V_0}R_0 = \pi/(2\sqrt{2})$ is the minimum square well potential size that can hold the first excited state and for the nth excited state is $\xi = n\pi/2\sqrt{2}$ with $n = 1, 2, 3\ldots$ and ξ being the reduced impurity size. The maximum number of atoms that the well can trap is proportional to the non-linear coupling term, $g^n_{\max}$. We have reported analytical expressions for $g^n_{\max}$ when the ground state and first excited states are at the threshold of de-localization, respectively.

Similarly, a square well potential coupled to a contact impurity (delta function) at the origin has been considered. The presence of the contact impurity has an effect on the behavior of the wave function at the origin and on the maximum number of atoms that the well can hold. When the delta impurity is repulsive, the number of trapped atoms is lower than the pure impurity square well potential. In all cases, the behavior for $\xi \gg 1$ is as predicted by the Thomas-Fermi approximation.

Finally, the width of the wave-function and density profile are reported as a guide to determine how much the wave-packet spreads out at the de-localization threshold. We find that the first excited state is more compact that the ground state when a repulsive contact impurity at the center is considered for the same reduced impurity size, but with fewer particles. For small reduced impurity sizes, the pure square well potential has the maximum tunneling probability for the wave-function.

The authors acknowledge financial support from Grants PAPIIT IN-110-714 and SC15-1-IR-25 to RCT and IA-102-414, SC15-1-S-81, PE-106-615 to RMF and technical assistance from Reyes Garcia at the ICF-UNAM computer center. We would like to knowledge fruitful discussion with Victor Romero Rochin. We gratefully acknowledge Jocele Wild and S.A. Cruz for comments that greatly improved the manuscript. All authors contributed equally to the paper.

Appendix A: Gauss-Seidel numerical method

We have implemented the Gauss-Seidel (GS) method [26] to find the ground and first excited state solutions of the time-independent NLSE. In the GS method, the energy is evaluated given an *improved* solution on a numerical grid.

In our case the wave-function, evaluated in the kth grid point (i.e. when $\chi \to \chi_k$), $\bar\phi_k$, is replaced by $\bar\phi'_k$, where

$$\bar\phi'_k \approx (1-\tau_r)\bar\phi_k + \frac{\tau_r\left(\bar\phi_{k+1}+\bar\phi_{k-1}\right)}{2[1+(\bar V_k + 2\bar g\bar\phi_k^2/\xi-\eta)(\xi\Delta\chi)^2)]}, \quad (A.1)$$

where τ_r is the relaxation parameter that ensures convergence to the lowest energy state. Note here that the prime over $\bar\phi$ means an improved solution. In our case we take $\tau_r = 3/4$ as a compromise between convergence time and precision [26]. Also, note that we are solving equation (34), and that the boundary conditions are $\bar\phi_0 = 0$ and $\bar\phi_{N+1} = 0$.

The main computational challenge is to systematically increase $\bar{g}$ to find $\bar{g}_{\max}$ for a given ξ. Thus, the problem is reduced to a root search for which $\eta(\bar{g}_{\max}) = 0$ for a given ξ. As $\bar{g}$ is increased, the wave-function penetrates further into the classically forbidden region, until $\bar{g}_{\max}$ is reached; at that point the solution is no longer a localized wave-function [20]. To determine $\bar{g}_{\max}$ (and hence $N_{\max}$) numerically, it is required that the numerical grid be large enough to contain the very slow decay of the wave-function when $\bar{g}$ approaches $\bar{g}_{\max}$. Note, however, that we strictly use $\bar{\phi}(\pm\chi_{\max}) = 0$, meaning that we effectively have an artificial box with $V(\pm\chi_{\max}) \to \infty$. This means that our $\eta > 0$ scattering states are artificially constrained in a box and are always square integrable.

To ensure that the determined $\bar{g}_{\max}$ is accurate to the precision that we demand, the results need to be insensitive to the location of the boundary. In our case, we choose $\chi_{\max} = 500$ and $\Delta\chi = 0.01$. The $\bar{g}_{\max}$'s were determined by choosing the reduced impurity size ξ ranging from 0.01 to 100 and allocating 20 values in a log scale, commensurate with the physical parameters of a typical BEC experiment (as discussed above). In all cases, we have assumed convergence for a given $\bar{g}$, when η from one iteration to the next changed less than $\Delta\eta = 10^{-16}$. The $\bar{g}$ was then incremented until reaching $\eta = 0$. The initial amount of the increment of g was 1% of the TF approximation. When a positive value of η was obtained for a given g, a step back was performed and Δg was reduced in half, until we reached $\eta = 0$ from below.

References

1. *Bose-Einstein Condensation*, edited by A. Griffin, D. Snoke, S. Stringaro (Cambridge University Press, New York, 1995)
2. A.S. Parkins, D.F. Walls, Phys. Rep. **303**, 1 (1998)
3. F. Dalfovo, S. Giorgini, L.P. Pitaevskii, S. Stringari, Rev. Mod. Phys. **71**, 463 (1999)
4. H. Ott, J. Fortagh, G. Schlotterbeck, A. Grossmann, C. Zimmermann, Phys. Rev. Lett. **87**, 230401 (2001)
5. J. Reichel, W. Hänsel, T.W. Hänsch, Phys. Rev. Lett. **83**, 3398 (1999)
6. K. Brugger, T. Calarco, D. Cassettari, R. Folman, A. Haase, B. Hessmo, P. Krger, T. Maier, J. Schmiedmayer, J. Mod. Opt. **47**, 2789 (2000)
7. K. Henderson, C. Ryu, C. MacCormick, M.G. Boshier, New J. Phys. **11**, 043030 (2009)
8. J. Fortágh, C. Zimmermann, Rev. Mod. Phys. **79**, 235 (2007)
9. A.D. Cronin, J. Schmiedmayer, D.E. Pritchard, Rev. Mod. Phys. **81**, 1051 (2009)
10. A.E. Leanhardt, A.P. Chikkatur, D. Kielpinski, Y. Shin, T.L. Gustavson, W. Ketterle, D.E. Pritchard, Phys. Rev. Lett. **89**, 040401 (2002)
11. M. Jääskeläinen, S. Stenholm, Phys. Rev. A **66**, 023608 (2002)
12. T. Lahaye, P. Cren, C. Roos, D. Guéry-Odelin, Commun. Nonlin. Sci. Numer. Simul. **8**, 315 (2003)
13. P. Leboeuf, N. Pavloff, S. Sinha, Phys. Rev. A **68**, 063608 (2003)
14. M. Koehler, M.W.J. Bromley, B.D. Esry, Phys. Rev. A **72**, 023603 (2005)
15. P. Leboeuf, N. Pavloff, Phys. Rev. A **64**, 033602 (2001)
16. M.W.J. Bromley, B.D. Esry, Phys. Rev. A **68**, 043609 (2003)
17. M.W.J. Bromley, B.D. Esry, Phys. Rev. A **69**, 053620 (2004)
18. T. Ernst, J. Brand, Phys. Rev. A **81**, 033614 (2010)
19. G.L. Gattobigio, A. Couvert, B. Georgeot, D. Guéry-Odelin, New J. Phys. **12**, 085013 (2010)
20. L.D. Carr, K.W. Mahmud, W.P. Reinhardt, Phys. Rev. A **64**, 033603 (2001)
21. R. Cabrera-Trujillo, M.W.J. Bromley, B.D. Esry, `arXiv:1202.4801v1` (2012)
22. B.T. Seaman, L.D. Carr, M.J. Holland, Phys. Rev. A **71**, 033609 (2005)
23. G. Baym, C.J. Pethick, Phys. Rev. Lett. **76**, 6 (1996)
24. E. Kamke, *Differentialgleichungen, lösungsmethoden und lösungen* (Leipzig, 1959)
25. M. Abramowitz, I.A. Stegun, *Handbook of Mathematical Functions* (Dover, New York, 1972)
26. S.E. Kooning, D.C. Meredith, *Computational Physics, FORTRAN version* (Perseus Books, Reading, MA, USA, 1990)
27. M.H. Anderson, J.R. Ensher, M.R. Matthews, C.E. Wieman, E.A. Cornell, Science **269**, 198 (1995)